Development 139, 2477-2487 (2012) doi:10.1242/dev.077214

Regulated temporal-spatial astrocyte precursor cell proliferation involves BRAF signalling in mammalian spinal cord

An-Chi Tien[1,*], Hui-Hsin Tsai[1,*], Anna V. Molofsky[1], Martin McMahon[2], Lynette C. Foo[3], Aparna Kaul[4], Joseph D. Dougherty[5,‡], Nathaniel Heintz[5], David H. Gutmann[4], Ben A. Barres[3] and David H. Rowitch[1,§]

SUMMARY

Expansion of astrocyte populations in the central nervous system is characteristic of evolutionarily more complex organisms. However, regulation of mammalian astrocyte precursor proliferation during development remains poorly understood. Here, we used Aldh1L1-GFP to identify two morphologically distinct types of proliferative astrocyte precursors: radial glia (RG) in the ventricular zone and a second cell type we call an 'intermediate astrocyte precursor' (IAP) located in the mantle region of the spinal cord. Astrogenic RG and IAP cells proliferated in a progressive ventral-to-dorsal fashion in a tight window from embryonic day 13.5 until postnatal day 3, which correlated precisely with the pattern of active ERK signalling. Conditional loss of BRAF function using BLBP-cre resulted in a 20% decrease in astrocyte production, whereas expression of activated *BRAF^{V600E}* resulted in astrocyte hyperproliferation. Interestingly, BRAF^{V600E} mitogenic effects in astrocytes were restricted, in part, by the function of *p16^{INK4A}-p19^{ARF}*, which limited the temporal epoch for proliferation. Together, these findings suggest that astrocyte precursor proliferation involves distinct RG and IAP cells; is subjected to temporal and spatial control; and depends in part on BRAF signalling at early stages of mammalian spinal cord development.

KEY WORDS: Astrocyte precursor, Glioma, RAS signalling, BRAF, Spinal cord development, Aldh1L1, Mouse

INTRODUCTION

Astrocytes are the most numerous cells in the mammalian central nervous system (CNS), yet much remains to be learned about their developmental and functional characteristics and regulation (Kettenmann and Ransom, 2005; Rowitch and Kriegstein, 2010). The dramatic increase in the number and complexity of glia during the course of evolution points to a role for astrocytes in the evolution of more complex neurological function. For example, in *Caenorhabditis elegans*, neurons outnumber glia by 6:1, whereas in the human brain there are equivalent numbers or more astrocytes than neurons (Nedergaard et al., 2003; Herculano-Houzel, 2009). Furthermore, there are clear differences in glial complexity in *Drosophila*, rodent and human brain; the human brain is characterised by significantly larger astrocytes with more elaborate processes than their rodent counterparts (Oberheim et al., 2009). Although tight regulation of astrocyte numbers is no doubt an important feature of CNS development, regulation of astrocyte precursor expansion is poorly understood. In addition, the issue of developmental regulation of astrocyte proliferation could also be of significance to human cancer, because astrocytes and their precursors are considered to be candidate cells-of-origin for astrocytoma, the most common type of adult malignant brain cancer (Stiles and Rowitch, 2008; Alcantara Llaguno et al., 2009).

During mouse spinal cord development, the process of neurogenesis and oligodendrogenesis is tightly controlled, both spatially and temporally. The developmental epoch for neurogenesis in the ventral neural tube is completed by approximately embryonic day (E) 12 (Lee and Jessell, 1999), at which time several early glial markers can be identified in the radial glia of the ventricular zone (VZ), including SOX9 (Stolt et al., 2003), NFIA and NFIB (Deneen et al., 2006), which are required for gliogenesis. Whereas oligodendrocytes are generated from defined ventral and dorsal domains in the embryonic VZ (Ligon et al., 2006), astrocytes have been proposed to arise throughout the dorsal-ventral axis of the spinal cord (Pringle et al., 1998), although this point is contentious (Agius et al., 2004).

In the spinal cord, astrocytes fall into two broad classes, fibrous and protoplasmic, based on (1) their location in white or grey matter, respectively, (2) morphology and (3) expression of glial filaments. Fibrous astrocytes typically express high levels of glial fibrillary acidic protein (GFAP), whereas protoplasmic astrocytes exhibit low or no GFAP expression. By contrast, several studies have suggested that the markers ID3, ALDOC (Aldo-C) and transgenic reporter lines for *Aldh1L1-GFP* can be used to identify fibrous and protoplasmic astrocytes in mature CNS (Bachoo et al., 2004; Muroyama et al., 2005; Cahoy et al., 2008; Doyle et al., 2008). However, whether they can be used to monitor committed astrocyte precursors at early developmental time points in spinal cord is less clear.

Here, we have extensively characterised Aldh1L1-GFP-positive cells during spinal cord development, commencing at the time when embryonic radial glia become committed to gliogenesis.

[1]Departments of Pediatrics and Neurosurgery, Eli and Edythe Broad Center of Regeneration Medicine and Stem Cell Research and Howard Hughes Medical Institute, University of California San Francisco, 513 Parnassus Avenue, San Francisco, CA 94143, USA. [2]Helen Diller Family Comprehensive Cancer Center, 1450 Third Street, University of California, San Francisco, CA 94158, USA. [3]Department of Neurobiology, Stanford University, Palo Alto, CA 94305 USA. [4]Department of Neurology, Washington University School of Medicine, St Louis, MO 63110, USA. [5]The Rockefeller University, 1230 York Ave, New York, NY 10065, USA.

*These authors contributed equally to this work
‡Present address: Department of Genetics & Department of Psychiatry, Washington University School of Medicine, St Louis, MO 63110, USA
§Author for correspondence (rowitchd@peds.ucsf.edu)

Accepted 29 April 2012

Using various markers of dividing cells, we found that proliferation of astrocyte progenitors is restricted to late embryonic-early neonatal stages, a very different expansion profile from that of oligodendrocyte populations. Moreover, we identify putative Aldh1L1-GFP-positive astrocyte intermediate precursor cells that derive from radial glia, migrate from the VZ to the mantle zone and lose radial glial morphology. As these cells undergo additional rounds of cell division, we suggest that they are transient amplifying progenitors, a novel stage of the lineage necessary for astrocyte expansion. Surveying core mitogenic pathways commonly involved in human brain cancer (The Cancer Genome Atlas Research Network, 2008), we identified that activation of RAS/RAF/ERK signalling correlated well with the proliferation phase of astrocytes. Indeed, using transgenic mice with modified alleles of *Braf*, encoding a RAF isoform that is expressed in the developing nervous system, we show that BRAF signalling is both necessary and sufficient to promote astrocyte proliferation. Finally, we show that $BRAF^{V600E}$ expression in spinal cord precursors is opposed by temporally regulated changes in signalling and cell cycle regulatory mechanisms, including $p16^{Ink4a}$ and $p19^{Arf}$, that delimit the mitogenic activity of BRAF during spinal cord development and function to regulate astrocyte numbers. Together, these findings indicate that temporal-spatial regulation of astrocyte precursor proliferation is tightly controlled and involves BRAF signalling in the mammalian spinal cord.

MATERIALS AND METHODS

Transgenic animals

Aldh1L1-GFP transgenic mice were generated by the GENSAT project (Gong et al., 2003; Heintz, 2004). The same methods and BAC technology (Gong et al., 2003; Heintz, 2004) we used to generate *Aldh1L1-cre* mice, with additional steps to remove LoxP sites from BAC as described (Gong et al., 2007); this line is maintained on an outbred background. We used mice that carry a conditional $Braf^{lox/lox}$ allele in which exon 12 of *Braf* is flanked by two *lox* sites, resulting in a product protein after cre exposure that is unstable (Chen et al., 2006). *Blbp-lacZ-cre* and *hGFAP-cre* transgenic mice that target embryonic radial glia and astrocytes, respectively, have been described (Hegedus et al., 2007). The conditional $Braf^{CA}$ mutant floxed allele (also known as $Braf^{tm1Mmcm}$) has been described previously (Dankort et al., 2007).

Thymidine analogue labelling

For thymidine labelling, the timed pregnant dams or pups were injected intraperitoneally with bromodeoxyuridine (BrdU, BD Pharmingen) or 5-ethynyl-2′-deoxyuridine (EdU, Invitrogen) at 50 μg/g body weight. The detailed injection timetables are indicated in the figures.

Tissue preparation and immunohistochemistry

All mice were perfused intracardially with 4% (w/v) paraformaldehyde and the spinal cords were post-fixed overnight and processed for cryosectioning at 14 μm thickness. For antibody staining, the sections on Superfrost Plus slides were air-dried, heated for antigen retrieval for 2 minutes and permeabilised with 0.2% Triton X-100/PBS and incubated with primary antibody overnight. Primary antibodies used in this study were: chick anti-GFP (1:1000, Aveslab), rabbit anti-OLIG2 (1:20,000, from lab stocks), rabbit anti-GFAP (1:500, DAKO), mouse anti-NeuN (1:100, Chemicon), goat anti-ALDOC (1:50, Santa Cruz Biotechnology), rabbit anti-BLBP (1:500, Millipore), mouse anti-nestin (1:500, Chemicon), mouse anti-vimentin (1:100, Developmental Studies Hybridoma Bank), rabbit anti-GLAST (1:500) and rat anti-BrdU (1:400, Novus Biologicals). Slides were then incubated with fluorescently labelled secondary antibodies (Invitrogen) and mounted with Fluoromount G with DAPI (SouthernBiotech). EdU incorporation was detected using the Click-iT Imaging Kit according to the manufacturer's instructions (Invitrogen). Sections with BrdU incorporation were pretreated with 2N HCl for 15 minutes at 50°C followed by rinses with 0.1 M boric acid (pH 8.0) prior to permeabilisation.

Image acquisition, analysis and cell counts

Fluorescence photomicrographs were collected with SPOT II camera/Nikon Eclipse 600 or Leica SP5 confocal microscopes. Images were processed and merged using Adobe Photoshop CS2 (Adobe). Cell counts were obtained from sections of upper thoracic spinal cord. For all counts performed, data reported represents data from greater than two animals and greater than three sections/animal, counted manually after imaging. Counts of thymidine analogue (EdU or BrdU)-incorporating cells were expressed as percentage of analogue+GFP+ cells of total Aldh1L1-GFP cells. Three hemisections of spinal cord from more than two animals for each genotype were counted without choosing any particular region. Particularly for the mitotic index calculation, owing to low percentage (1-3%), the number of Aldh1L1-GFP+ cells counted is from four to six sections per animal, from three independent animals (except E14.5, in duplicate). For regional astrocyte number quantification, distributions of those cells in dorsal (D), intermediate (I) and ventral (V) spinal cord were obtained by drawing a straight line through the midline and further dividing half of spinal cord into three regions, each encompassing an arc of 60° using the central canal as the origin. The distribution was counted as percentage of analogue+ GFP+ cells in each region in total analogue+ GFP+ cells. All counts were expressed as average ± s.d. Student's *t*-test was used for statistical analysis of significance.

Astrocyte culture

The astrocyte culture was performed following a standard method (McCarthy and de Vellis, 1980) with modifications. Briefly, the forebrains from postnatal day (P) 1 animals were isolated and dissociated with 0.0125% trypsin for 30 minutes. The tissue was triturated with a Pasteur pipette for dissociation and plated on poly-D-lysine-coated plates with 10% serum in DMEM/F12 (Invitrogen) medium. After 4 days, the oligodendrocytes were shaken off to obtain the astrocyte culture and 5×10^4 cells/ml were then re-plated in DMEM/F12 + 10 ng/ml epidermal growth factor (EGF) + 10 ng/ml fibroblast growth factor (FGF) to maintain immature property of the astrocytes. The growth curve was calculated every other day after plating.

Flow cytometry and qPCR

Spinal cords from Aldh1L1-GFP transgenic animals were papain-dissociated and flow-cytometrically sorted as previously described (Cahoy et al., 2008). RNA isolation and qPCR was performed as previously described (Molofsky et al., 2003). Briefly, Aldh1L1-GFP positive cells were double sorted with purity >95%. RNA was isolated using trizol reagent and DNase digested. RNA was reverse transcribed using random hexamers. qPCR was performed on a Roche light-cycler and normalised to β-actin. The EGFR primers are 5′-TCTGCCACCTATGCCACGCC-3′ and 5′-GCCACCCACAATCCCAGTGGC-3′.

RESULTS

Evidence that Aldh1L1-GFP expression commences in gliogenic radial glia and astrocytes in developing mouse spinal cord

In order to identify proliferating radial glia, protoplasmic and fibrous astrocytes, we assessed expression of the candidate markers Aldh1L1 (Cahoy et al., 2008), Id3 (Muroyama et al., 2005) and Aldo-C (Bachoo et al., 2004) using transgenic reporters or antibody-mediated labelling. As shown (Fig. 1A-D), the Aldh1L1-GFP reporter segregates from NeuN (RBFOX3 – Mouse Genome Informatics)-positive neurons and most OLIG2-positive cells (Fig. 1A,B), which primarily marks oligodendroglia in the spinal cord (2% co-labelling with OLIG2 was observed). By contrast, Aldh1L1-GFP+ cells co-labelled extensively with GFAP-positive fibrous astrocytes in white matter (Fig. 1C, dashed line). Whereas GFAP expression is relatively low in protoplasmic grey matter astrocytes, ALDOC expression is robust in grey matter protoplasmic astrocytes and exhibits extensive colocalisation with Aldh1L1-GFP (Fig. 1D). Further analysis with FACS sorting indicates that Aldh1L1-GFP-positive cells are mostly GFAP-

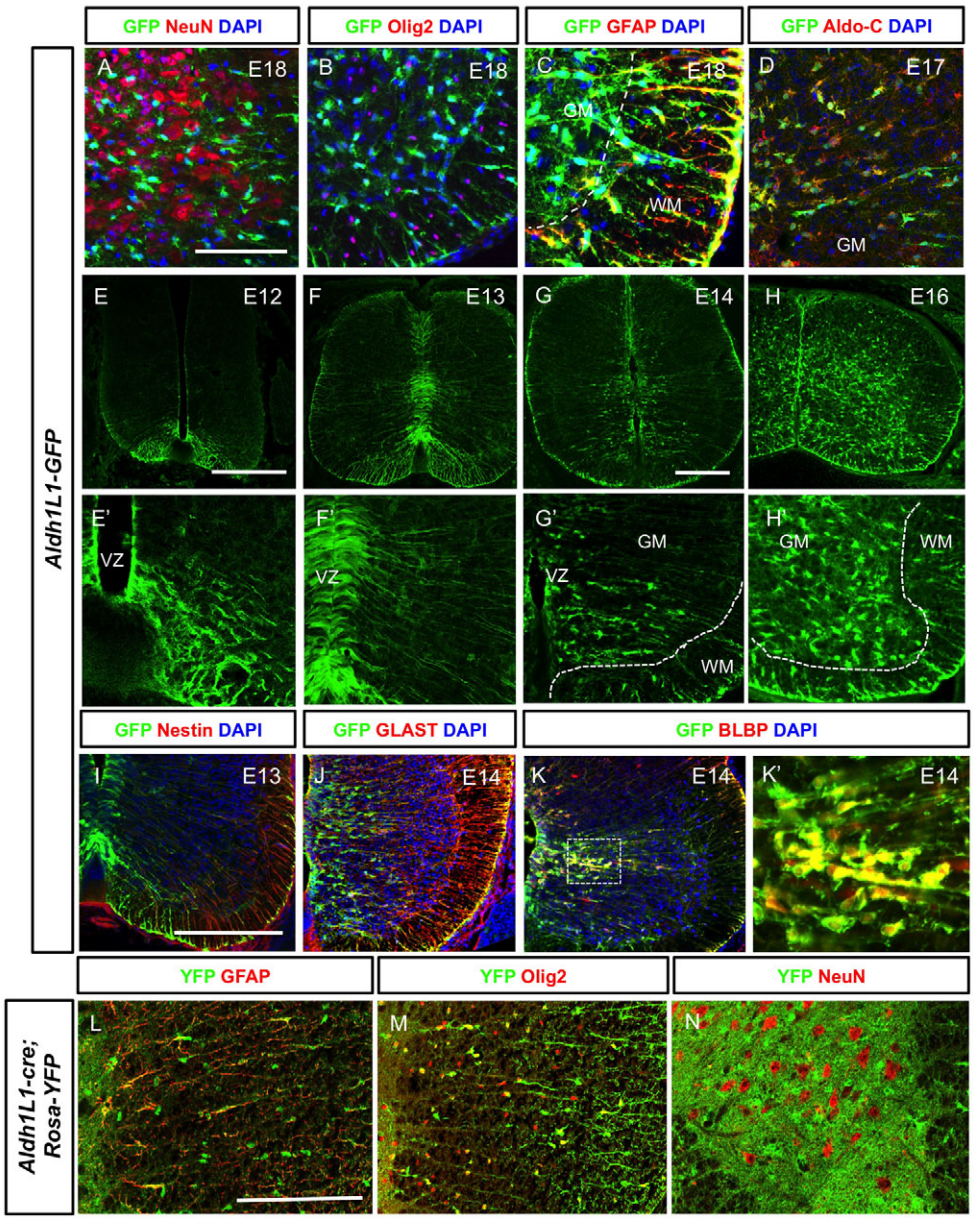

Fig. 1. Expression profile of Aldh1L1-GFP labels gliogenic radial glia and astrocytes during spinal cord development. (**A-H'**) Spinal cord sections of Aldh1L1-GFP transgenic mice. (A-D) Aldh1L1-GFP+ cells at E18 do not colocalise with NeuN+ neurons (A) or strong OLIG2+ oligodendrocytes (B). Aldh1L1-GFP+ cells at this stage express astrocyte markers including GFAP and ALDOC in the WM (white matter) and GM (grey matter), respectively (C,D). The dashed line indicates the boundary between WM and GM. (E-H) Developmental expression profile of Aldh1L1-GFP+ cells in the spinal cord and higher magnification pictures are shown (E′-H′). At E12, Aldh1L1-GFP+ cells are localised at ventral VZ (E,E′) and extend their process to the ventral pial surface. At E13, the presence of Aldh1L1-GFP+ cells extends to entire VZ and cells also establish processes to the dorsal pial surface (F,F′). However, not until E14 when the migration of Aldh1L1-GFP+ cells can be observed prominently at ventral domain of the spinal cord (G,G′). At E16, Aldh1L1-GFP+ cells populate the entire spinal cord in both GM and WM (H,H′). The dashed lines (G′,H′) indicate the boundary between GM and WM. (**I-K'**) Early stages of Aldh1L1-GFP+ cells express some radial glial markers including nestin (red in I), GLAST (red in J) and BLBP (red in K) before and after they migrate out from VZ. Note that the staining outside of spinal cord for nestin and GLAST (I,J) are meninges and considered to be non-specific. In K and K′, BLBP exhibits extensive colocalisation of Aldh1L1-GFP+ cells (higher magnification in K′). (**L-N**) Fate mapping analyses of *Aldh1L1-cre; Rosa-YFP* spinal cords (n=5 independent animals) show extensive colocalisation of fate-mapped progeny with glia. Seventy-five percent express GFAP (L) and 15% of cells co-express OLIG2 (M) whereas only 10% express NeuN (N), indicating Aldh1L1-cre expression commences in radial glia at about the onset of gliogenesis in spinal cord. Scale bars: 100 μm for A-D; 200 μm for E-N.

positive in P6 spinal cord (supplementary material Fig. S1), confirming co-expression of GFAP in Aldh1L1-GFP-positive cells. Morphological evidence was also used to confirm protoplasmic astrocyte identity of Aldh1L1-GFP-positive cells (H.-H.T. and D.H.R., unpublished observations).

In contrast to the relatively late onset of GFAP expression (~E18), we observed that Aldh1L1-GFP expression commenced at E12.5 in the ventral neural tube (Fig. 1E,E′). At E13.5 (Fig. 1F,F′), expression of Aldh1L1-GFP extends to the pial surface but is restricted to cells with nuclei that line up in the ventricular zone, a typical morphology

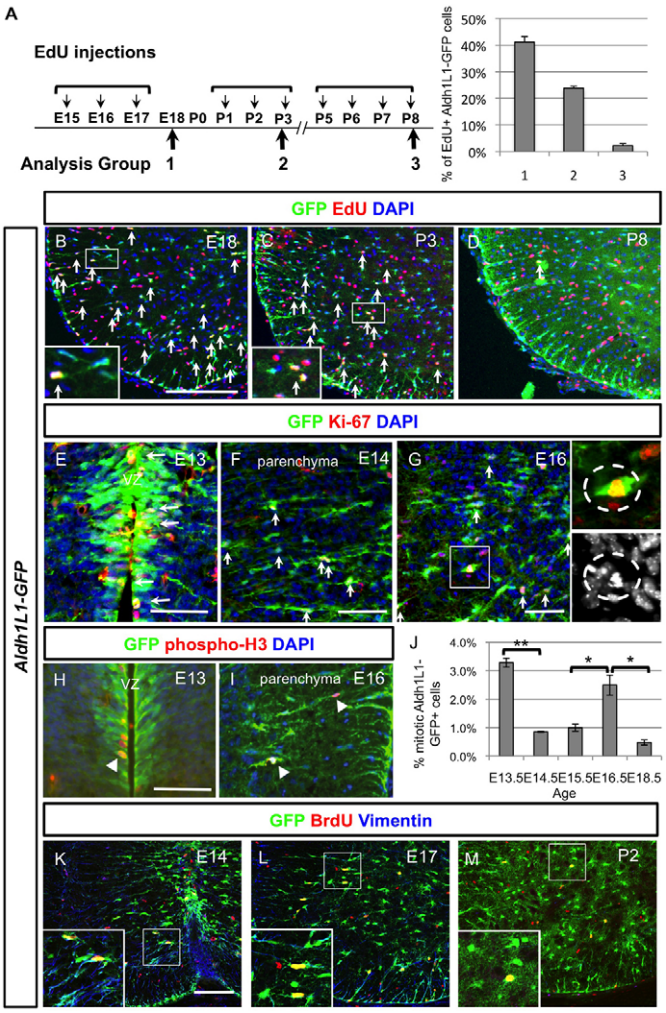

Fig. 2. Characterisation of astrocyte proliferation at various stages of development and identification of the intermediate astrocyte progenitors (IAPs). (**A**) Timetable of the thymidine analogue EdU administration at three developmental time periods (E15-17, P1-3 and P5-8) and quantification of EdU+ Aldh1L1-GFP+ cells at these three stages obtained by counting spinal cord hemisections (*n*=3). Note that the detailed number is listed in supplementary material Table S1. (**B-D**) Spinal cord sections from these three different EdU tracing experiments are shown and EdU+ Aldh1L1-GFP+ are indicated with arrows. Note that the ones that were picked as positive ones are indicated in the higher power picture. (**E-G**) At E13 (E), Aldh1L1-GFP+ cells are proliferating at the VZ and labelled with Ki-67 in red (marked by arrows). After this, Aldh1L1-GFP+ cells migrate out from VZ and reside in the parenchyma at E14 (F) or E16 (G), some of them can be labelled with proliferation marker Ki-67 (indicated with arrows) and we have termed these cells intermediate astrocyte progenitors (IAPs). The mitotic cells can also be observed (indicated in the insets) among these IAPs. DAPI staining is used to identify the chromosomal condensation of a typical mitotic cell. (**H-J**) Colocalisation of mitotic marker phospho-histone 3 with Aldh1L1-GFP+ cells is observed in VZ at E13 (H) and parenchyma at E16 (I) (indicated by arrowheads). Quantification of mitotic Aldh1L1-GFP+ cells represents the average of triplicate samples from all ages except E14.5 (duplicate), with four to six sections counted per animal. Graph shows average ± s.e.m., statistics calculated using ANOVA. **P*<0.05, ***P*<0.01. (**K-M**) By acute BrdU labelling during the proliferative period, Aldh1L1-GFP cells express some radial characteristics (vimentin in blue) at early time points (E14 and E17) whereas fewer Aldh1L1-GFP+ cells are proliferating at postnatal stage and did not express vimentin. Scale bars: 200 μm in B; 50 μm in E-H; 100 μm in K.

of radial glial cells (Fig. 1F,F′). Beyond E14 (Fig. 1G-H′), Aldh1L1-GFP-expressing cells can be found in the parenchyma, suggesting that astrocytes start to migrate out from the VZ and populate the lateral spinal cord at these stages. Furthermore, we found that the radial glial markers, including nestin, GLAST (SLC1A3 – Mouse Genome Informatics) and BLBP (FABP7 – Mouse Genome Informatics), showed extensive colocalisation with Aldh1L1-GFP cells at early embryonic stages (Fig. 1I-K). Finally, we used *Aldh1L1-cre* transgenic mice to fate map progenitors. As shown (Fig. 1L-N), crosses with the *ROSA26-YFP* conditional reporter (Zambrowicz et al., 1997) revealed that progeny co-labelled with markers of astrocytes, and some oligodendrocytes but segregated mostly from the neuronal marker NeuN (~10%). Together, these findings indicate that Aldh1L1-driven expression commences in radial glia that are committed to gliogenesis (i.e. after the major period of neuronal production) and that it continues to mark the astrocyte lineage at least until at least P28.

Bi-modal proliferation profile of Aldh1L1-GFP-positive cells during spinal cord development

Although previous findings in the optic nerve (Skoff et al., 1976) and spinal cord (Barnabé-Heider et al., 2010) suggest that embryonic progenitors contribute significantly to long-term stable populations of astrocytes, the proliferation profile for embryonic astrocyte precursors is poorly characterised owing to lack of markers that capture early developmental stages. Because the Aldh1L1-GFP permits identification of gliogenic radial glia, fibrous and protoplasmic astrocytes, we used this marker to characterise the proliferation profile of embryonic and neonatal astrocyte precursors.

To determine the major developmental epoch(s) of Aldh1L1-GFP cellular proliferation, we used several approaches (Fig. 2; supplementary material Fig. S2). First, we performed injections of thymidine analogues at different developmental time periods and assessed Aldh1L1-positive populations retaining thymidine analogues between P15 and P18 (supplementary material Fig. S2). This showed that ~20-30% of astrocytes have undergone proliferation during these early developmental time points (E15-18, P0-2). Observations following the early injection regimes contrasted with those following late (P10-14) thymidine analogue injections, which captured <1% of the mature astrocytes, as well as the ongoing and robust proliferation observed in the oligodendrocyte lineage. These results suggest that most astrocytes precursors exit the cell cycle between E15 and P3.

Having defined the major epoch and contribution of Aldh1L1+ cell proliferation to stable astrocyte populations at two weeks of postnatal age, we next examined acute astrocyte precursor proliferation during the time windows E15-17, P1-3 and P5-8. Pups or pregnant dams were injected with EdU once per day for 3-4 days and subjects were sacrificed and analysed 2 hours after the final injection (Fig. 2A). As shown (Fig. 2A-C), 40% and 30% of Aldh1L1-GFP+ cells incorporated EdU (labelled with arrows) after injection from E15-17 and P1-3, respectively, whereas <5% of cells were labelled after EdU injection from P5-8 (Fig. 2D). Moreover, when P25 mice were injected with EdU (daily for 5 days) no EdU-positive Aldh1L1-GFP cells were identified in the spinal cord (data not shown). Together, these findings indicate that Aldh1L1-GFP cells in the spinal cord proliferate largely from ~E15 to P3.

Evidence that radial glia and intermediate astrocyte precursors (IAPs) give rise to astrocytes

It is generally accepted that astrocytes are derived from radial glia in the VZ (Schmechel and Rakic, 1979; Barry and McDermott, 2005). However, the finding of proliferative Aldh1L1-GFP cells between

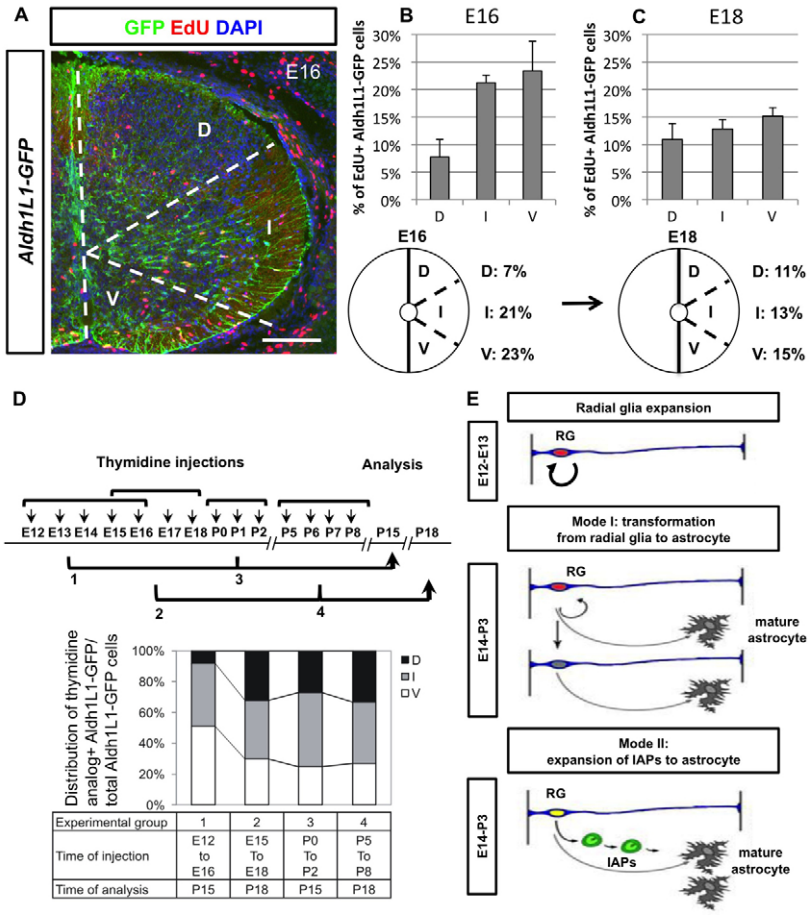

Fig. 3. Proliferation of Aldh1L1-GFP+ cells progresses from ventral/intermediate domains to dorsal domain. (**A**) Half of the spinal section is divided into three regions (indicated by dashed lines): dorsal (D), intermediate (I) and ventral (V) domains. (**B**,**C**) Quantification of proliferative EdU+ Aldh1L1-GFP+ cells in each domain at E16 and E18 was obtained from three sections from three independent animals. Note that proliferating Aldh1L1-GFP+ cells in the dorsal domain is significantly less compared with intermediate/ventral domains at E16. Error bars represent s.d. (**D**) Experimental design of labelling astrocytes by thymidine analogue injections. EdU was injected antenatally and BrdU was injected postnatally to save the number of animals used in the study and hence there were four experimental groups. Each group was analysed at later postnatal ages and three animals were analysed in each group. Quantification of thymidine analogue+ Aldh1L1-GFP+ cells in dorsal, intermediate and ventral domains showed that the dorsal domain gave rise to a much lower percentage of astrocytes before E16. (**E**) Model of astrocyte proliferation profile in the spinal cord. The radial glia (RG) proliferate extensively at early phase (E12-13) whereas the intermediate astrocyte precursor cells proliferate at a later phase (E14-P3). Two modes of astrogenesis are proposed. Scale bar: 200 μm.

E15 and P3 in the mantle region of the spinal cord (Fig. 2A-D) was consistent with the existence of a non-radial glial proliferative type of transient-amplifying progenitor, akin to those observed in forebrain subventricular zone (SVZ). We examined proliferative Aldh1L1-GFP+ cells using Ki-67 or an acute pulse of EdU labelling (1 hour before sacrifice) at various stages from E13.5 to E18.5. As shown (Fig. 2E), at E13.5 most Aldh1L1-GFP cells possess radial glial morphology with nuclei lined up in register with the VZ and many of these were observed to be Ki-67-positive (indicated by arrows). At E14.5, when Aldh1L1-GFP cells start to migrate out from the VZ, we observed that ~25% nuclei in the parenchyma co-labelled with Ki-67 (Fig. 2F, arrows). However, we observed few mitotic figures in such nuclei at this stage. By contrast, at E15-16 we observed that ~40% of proliferating Ki-67+ Aldh1L1-GFP+ cells were located in the parenchyma and ~2% of them showed mitotic features (Fig. 2G). To quantify the mitotic Aldh1L1-GFP+ cells further, we used anti-phospho-histone3 (pH3) to label mitotic cells at late embryonic stages (E13-18). As shown (Fig. 2H), ~3% of Aldh1L1-GFP+ radial glia in the VZ/SVZ undergo mitosis at E13.5 whereas the major population of mitotic Aldh1L1-GFP+ cells at E16.5 are located in the parenchyma (Fig. 2I,J). These results suggest that after radial glia derivatives migrate out from the VZ, they can, and often do, undergo additional rounds of cell division in the parenchyma to generate astrocytes. We therefore termed this type of proliferative astrocyte precursors 'intermediate astrocyte precursors' (IAPs).

Despite their parenchymal location, distinct from typical radial glia whose nuclei align along the VZ, putative Aldh1L1-GFP+ IAPs continue to express some radial glia markers. For example, vimentin labelling between E14 and E17 captured proliferative Aldh1L1-GFP cells with nuclei in the parenchyma (Fig. 2K-M). Conversely, vimentin is largely absent in Aldh1L1-GFP cells at P2 when the majority of cells are quiescent. Together, these data suggest that proliferative IAPs located in the mantle region retain a pattern of vimentin expression that suggests an astroglial transition stage.

Proliferation of astrocyte precursors in the spinal cord follows a temporal ventral-to-dorsal progression

Because ventral pMN (progenitor motor neuron)-derived motor neurons and oligodendrocytes develop prior to dorsal neuron and oligodendroglial populations (Lee and Jessell, 1999; Rowitch and Kriegstein, 2010), we investigated whether there is a differential timing for IAP proliferation along the dorsoventral axis. To quantify this, we arbitrarily divided the spinal cord into three geometric areas to capture dorsal, intermediate and ventral progenitors (e.g. dashed lines in Fig. 3A, see Materials and methods). When a short pulse of EdU was administrated at E16, we found prevalent intermediate and ventral proliferating Aldh1L1-GFP cells compared with the dorsal domain (Fig. 3B). By contrast, at E18, the percentage of proliferating astrocytes showed no difference in any dorsoventral domain (Fig. 3C). This trend of dorsal astrocytes being proliferative at a later stage was confirmed by pulse-chase experiments. For instance, when results of early (E12-16) pulse-chase is examined at two weeks of age (P15-18), robust EdU-positive Aldh1L1-GFP cells were observed significantly more often in the intermediate and ventral domains versus the dorsal domain (Fig. 3D). By contrast, later pulse injections (E15-18) showed EdU-positive Aldh1L1-GFP cells in all

three domains. Based on these observations (Figs 1-3), we proposed that the nature of proliferating astrocyte precursors shift from radial glia cells at E12-13 to IAPs at E14-P3 (summarised in Fig. 3E and in Discussion). Together with their location shift from ventral to dorsal, this coincides with increasing developmental maturity during embryonic, foetal and neonatal stages.

Activation of ERK is correlated with proliferation of spinal cord Aldh1L1-GFP cells

After determining the proliferation profile of spinal cord Aldh1L1-GFP+ cells in temporal-spatial terms, we sought to examine the role of certain growth-related signalling pathways during astrocyte proliferation. We focused on the core signalling pathways RAS/RAF/ERK and PI3-K/mTOR, owing to their prominent roles in regulation of neural stem cell proliferation as well as human glioma (The Cancer Genome Atlas Research Network, 2008). We first investigated downstream targets of PI3-K, including phospho-AKT and phospho-S6 at E16, when there is robust proliferation of Aldh1L1-GFP cells. However, we did not observe any correlation of phospho-S6 or phospho-AKT expression with astrocyte proliferation (supplementary material Fig. S3). By contrast, we detected phospho-ERK1/2 (pERK1/2; phospho-MAPK3/MAPK1) proteins, a readout of active RAF signalling, in ~20-25% of Aldh1L1-GFP cells from E14 to P1 (Fig. 4A-C″; data not shown). At later stages (P6 and beyond), numbers of pERK1/2-Aldh1L1-GFP double-positive cells are greatly reduced (Fig. 4C-C″), suggesting that roles for RAS/RAF/ERK signalling are limited to astrocyte expansion not subsequent maturation.

Interestingly, we note that at early time points (e.g. E16) the levels of pERK1/2 protein appeared to be relatively high in the intermediate domain compared with the dorsal domain (domain boundary marked by dashed lines, Fig. 4A), correlating with the previously noted differential rates of proliferation in this domain. Indeed, we found that pERK1/2+ proliferating IAP-types cells are also Ki-67-positive in the intermediate domain at E16 (Fig. 4D-D″) compared with those in the dorsal domain that are both pERK1/2-negative and Ki-67-negative at this stage (Fig. 4E-E″). These data suggest potential roles for RAS/RAF signalling in regulation of astrocyte precursor proliferation.

BRAF function is necessary for astrocyte proliferation

Several components of the RAS/RAF/ERK signalling pathway have been shown to be important for neural development and are mutated in several human neurodevelopmental disorders. Whether this signalling pathway regulates astrocyte proliferation is unknown. We focused on BRAF because germ-line mutations of *BRAF* are found in cardio-facio-cutaneous (CFC) syndrome (Duesbery and Vande Woude, 2006; Niihori et al., 2006; Rodriguez-Viciana et al., 2006), whereas somatic $BRAF^{V600E}$ gain-of-function mutations are thought to be aetiological in paediatric glioma (Schiffman et al., 2010). To test a requirement for *BRAF* function, we intercrossed *Blbp-lacZ-cre* mice that express bacteriophage P1 cre recombinase in radial glia (Hegedus et al., 2007) to conditional $Braf^{lox/lox}$ mice, in which *loxP* sites flank *Braf* exon 12 encoding a key region of the BRAF protein kinase domain. Cre-mediated excision of *Braf* exon 12 was expected to result in a null allele that expresses no detectable BRAF protein (Chen et al., 2006); as shown (Fig. 5A), in *Blbp-lacZ-cre;* $Braf^{lox/lox}$ animals BRAF expression is almost eliminated in the spinal cord but not in the dorsal root ganglia (supplementary material Fig. S4A), indicating a successful cre targeting of *Braf* in the CNS using this strategy.

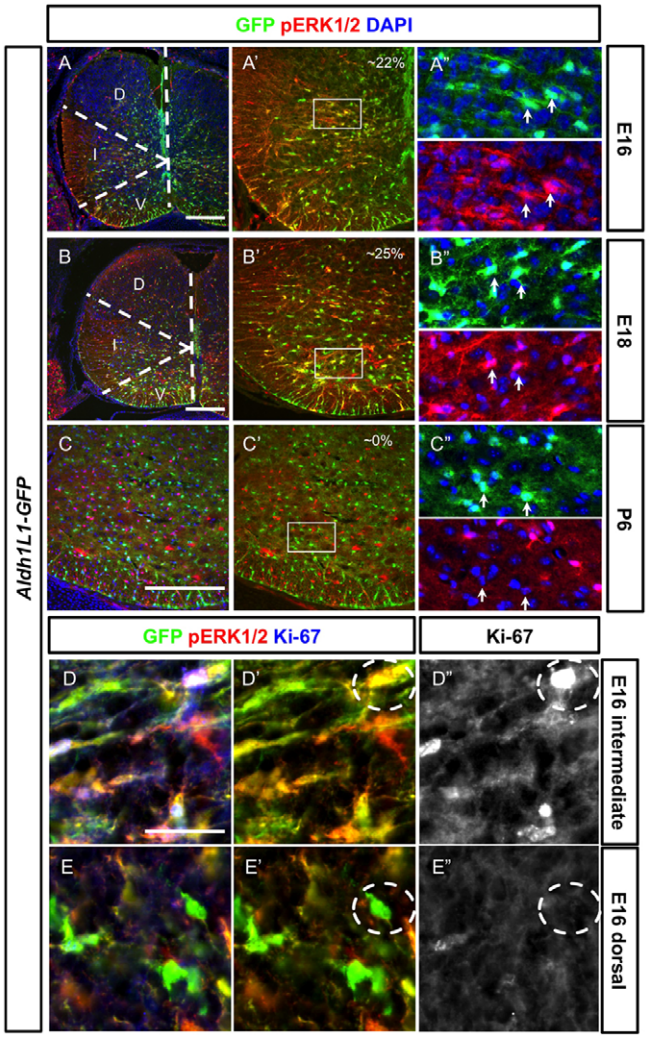

Fig. 4. Proliferative Aldh1L1-GFP+ cells in the parenchyma of the spinal cord are often co-labelled with activated ERK1/2. Spinal cord sections from different developmental stages are shown (developmental stages are indicated in the left boxes). (**A-C″**) Activated pERK1/2 (red) is found in the Aldh1L1-GFP+ cells (green) at E16 (A-A″) and E18 (B-B″) but not at P6 (C-C″). At E16 (A-A″), pERK1/2 is strongly expressed in the intermediate domain (indicated by the dashed line) but not in the dorsal domain whereas strong pERK1/2+ Aldh1L1-GFP+ cells can be identified in all three domains at E18 (B-B″). The colocalisation percentage of pERK1/2+ Aldh1L1-GFP cells among all GFP+ cells is indicated. At P6 (C-C″), expression of pERK1/2 in Aldh1L1-GFP is not observed. The boxed areas in A′-C′ are shown in A″-C″. Arrows indicate GFP+ cells. D, dorsal domain; I, intermediate domain; V, ventral domain. (**D-E″**) At E16, Aldh1L1-GFP+ cells in the intermediate domain can often be identified with pERK1/2+ and Ki-67+ (D-D″) whereas those in the dorsal domain have not undergone proliferation and express less pERK1/2 and are negative for Ki-67 (E-E″). Compare the dashed circles in D′ and E′. Scale bars: 200 μm in A-C; 40 μm in D.

To examine astrocyte proliferation in *Blbp-lacZ-cre;* $Braf^{lox/lox}$ animals, EdU+ Aldh1L1-GFP cells from different stages and regions were quantified compared with their non-mutant littermates. For early injections of EdU from E15 to E17, we found a significant decrease of EdU+ Aldh1L1-GFP cells in $Braf^{lox/lox}$ mutant animals for both intermediate and ventral domains when animals were analysed either at E18 or P8 (Fig. 5B-D). EdU

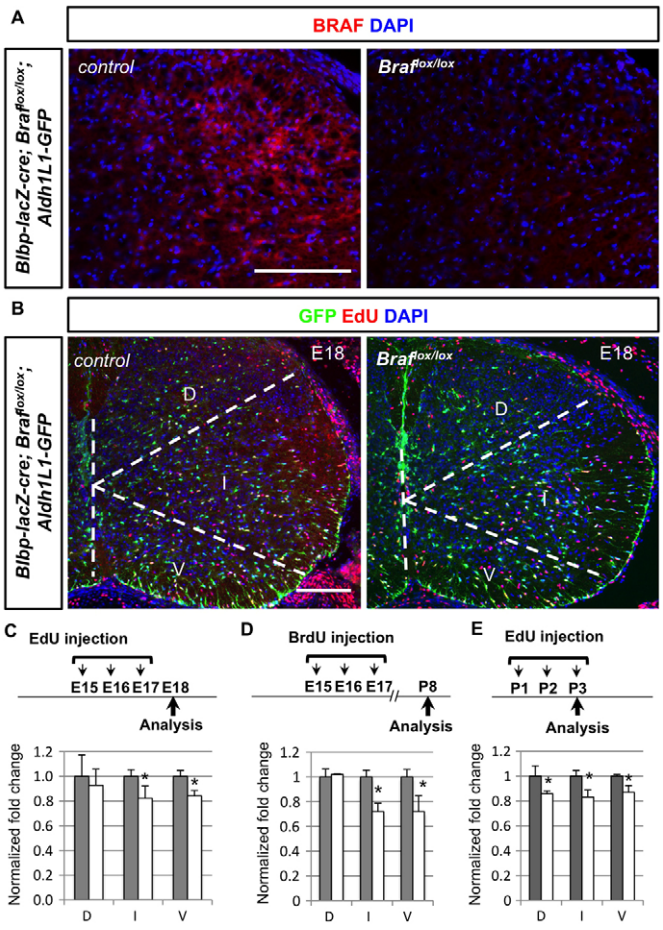

Fig. 5. Conditional deletion of *Braf* results in decrease proliferation of Aldh1L1-GFP+ cells. (**A**) BRAF expression (red) is largely absent in the *Blbp-lacZ-Cre; Braf*$^{flox/lox}$ spinal cords compared with littermate controls. (**B**) Decreased number of EdU+ (red) Aldh1L1-GFP+ (green) cells in the *Braf*$^{flox/lox}$ mutant animals compared with littermate controls. (**C**,**D**) Animals with EdU or BrdU injection timetable (E15-17) were analysed at E18 or P8, respectively. The percentage of EdU+ Aldh1L1-GFP+ cells among all GFP+ cells is quantified from three different domains, obtained from three independent animals. To obtain normalised fold change, percentage from control animals (grey bars) is set as 1 arbitrarily and a decrease in mutant animals is observed (white bars). Note that the detailed percentage and normalised number is included in supplementary material Table S1. (**E**) Animals with EdU injection protocols (P1-3) were analysed at P3 and the normalised fold change is shown as describe above. D, dorsal domain; I, intermediate domain; V, ventral domain. Scale bars: 100 μm.

injections from P1 to P3 indicate that the percentage of EdU+ Aldh1L1-GFP cells in *Braf*$^{flox/lox}$ mutant pups is significantly lower in all three domains compared with their littermates (Fig. 5E). These findings indicate that BRAF is involved in optimal levels of astrocyte proliferation during development.

Mutationally activated BRAF^{V600E} promotes astrocyte proliferation

To investigate whether gain-of-function BRAF was sufficient to promote astrocyte proliferation, we used the conditional knock-in *Braf*$^{CA/+}$ allele (Dankort et al., 2007), which expresses the highly active BRAF^{V600E} kinase mutant protein after cre exposure. Cre-mediated rearrangement of the *Braf*$^{CA/+}$ allele results in the expression of BRAF^{V600E} at normal physiological levels of expression under faithful control of endogenous cis-acting DNA regulatory sequences. BRAF^{V600E} promotes sustained activation of the MEK/ERK signalling pathway in cells.

Results from intercrosses of *Blbp-lacZ-cre* with *Braf*$^{CA/+}$ are shown in Fig. 6. From early injections of EdU (E15-17), we observed significantly increased number of EdU+ Aldh1L1-GFP cells in all three domains (Fig. 6A,B), indicating that BRAF^{V600E} is sufficient to promote hyperproliferation of astrocytes. Additionally, we observed widespread upregulation of pERK1/2 throughout the spinal cord (data not shown), confirming that BRAF^{V600E} activates ERK1/2 until E18.

We next investigated actions of BRAF^{V600E} to promote excessive proliferation of astrocyte radial glial and/or intermediate precursors. Specifically, we considered the possibilities that BRAF^{V600E} (1) promoted extra rounds of proliferation, (2) extended the window of precursor proliferation beyond P3, and/or (3) reduced levels of Aldh1L1-GFP+ cell apoptosis. At E16, acute labelling revealed increased levels of EdU+ Aldh1L1-GFP-positive cells in VZ and parenchyma (Fig. 6C), indicating that activated BRAF^{V600E} promotes proliferation for both the astrocytic radial glia and the putative intermediate astrocyte precursors. Next, we sought to examine the effect of BRAF^{V600E} in postnatal astrocyte proliferation. However, owing to perinatal lethality of *Blbp-lacZ-cre; Braf*$^{CA/+}$ mice, we used *hGFAP-cre; Braf*$^{CA/+}$ mice, which survive postnatally. As shown (Fig. 6D,E), we found significantly increased numbers of pERK1/2+ Aldh1L1-GFP cells at P1. We used EdU pulses again to examine the percentage of proliferative astrocytes at early postnatal stage and found that hyperproliferation of astrocytes at P1-3 is observed in *hGFAP-cre; Braf*$^{CA/+}$ animals (quantified in Fig. 6F). Finally, we observed no differences in levels of apoptosis at any stage studied (supplementary material Fig. S4B; data not shown). To confirm that cell-autonomous effects of BRAF^{V600E} cause increased proliferation of astrocytes, we cultured astrocytes from *hGFAP-cre; Braf*$^{CA/+}$ mice and found that indeed the astrocyte cultures from these mutant mice exhibit a robust increase in astrocyte number (supplementary material Fig. S4C). Together, these data indicate that BRAF^{V600E} promotes astrocyte proliferation during the normal astrocyte developmental epoch.

p16^{Ink4a} and p19^{Arf} function is required for temporal control of BRAF^{V600E}-driven proliferation

We examined next whether BRAF^{V600E} is sufficient to drive persistent astrocyte proliferation beyond the normal developmental window. We injected BrdU at P7 and examined the animals at P12 (Fig. 7A). Although the total number of astrocytes in all three domains is significantly increased (Fig. 7A,B), the number of proliferating BrdU+ Aldh1L1-GFP cells in *hGFAP-cre; Braf*$^{CA/+}$ animals is not significantly increased above littermate controls.

As shown above (Figs 2, 4), astrocytes after P3 cease proliferation and exhibit low pERK1/2 activity. Therefore, we examined whether BRAF^{V600E} promotes activated ERK1/2 at P3 and P6 in relatively mature astrocytes. Aldh1L1-GFP cells in *hGFAP-cre; Braf*$^{CA/+}$ mice at these stages did not show ectopic or persistent pERK1/2 staining compared with littermate controls in the spinal cord (supplementary material Fig. S4D). In addition, astrocyte proliferation at P6-8 and P13-15 assessed by EdU incorporation was unaffected (quantified in Fig. 7C), suggesting that BRAF^{V600E} does not promote astrocyte proliferation beyond the normal developmental epoch.

In other systems, BRAF^{V600E} promotes induction of tumor suppressors, including p16^{Ink4a} and p19^{Arf}, which lead to senescence (Lloyd et al., 1997; Michaloglou et al., 2005). To test

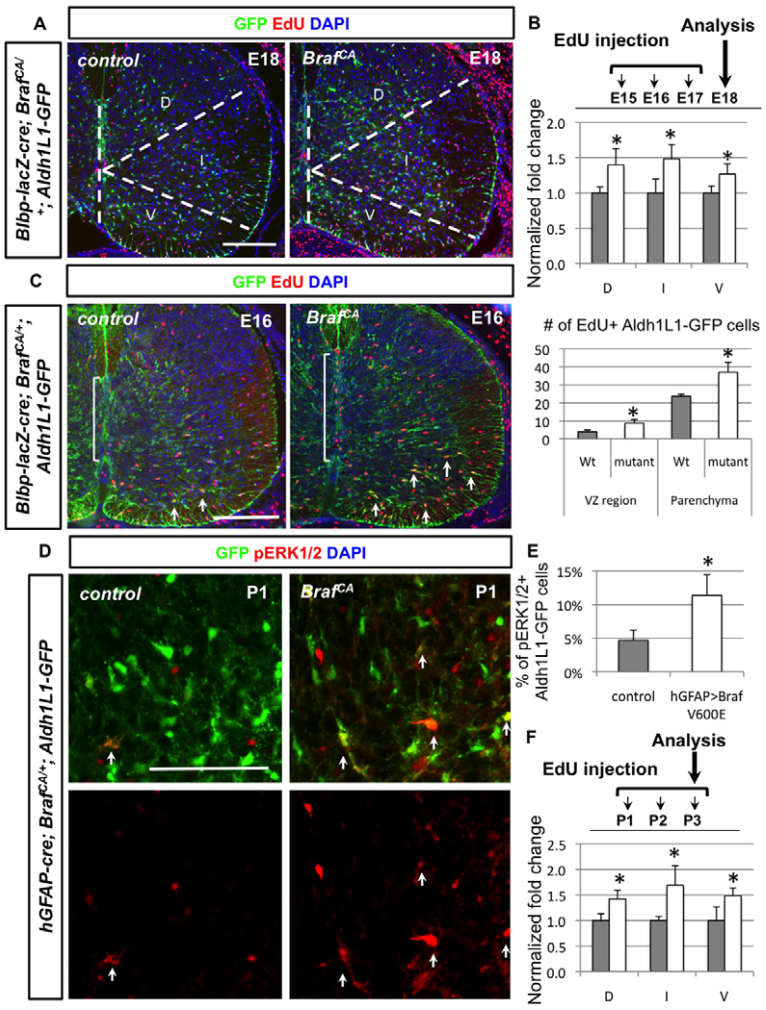

Fig. 6. Conditional activation of BRAF^{V600E} in radial glia at different stages results in overproduction of Aldh1L1-GFP+ cells. (**A**,**B**) At E18, *Blbp-lacZ-cre; Braf$^{CA/+}$* animals show increased EdU+ (red) Aldh1L1-GFP+ (green) cells in all three domains when EdU is injected from E15 to E17. The percentage of EdU+ Aldh1L1-GFP+ cells among all GFP+ cells in each domains is quantified (*n*=3 for each genotype). The percentage is then normalised by control and the control is arbitrarily set to 1 in the bar graph (B). Grey bars represent control whereas white bars are for mutant animals. (**C**) Colocalisation of EdU (red) and Aldh1L1-GFP+ (green) cells is examined in *Blbp-lacZ-cre; Braf$^{CA/+}$* animals with a short pulse of EdU injection 1 hour before perfusion. Both populations of Aldh1L1-GFP+ cells lining in the VZ (indicated by brackets) and in the parenchyma (indicated by arrows) show significantly increased number of EdU incorporations. The quantification of number of EdU+ Aldh1L1-GFP+ cells is shown in the bar graph. (**D**,**E**) In *hGFAP-cre; Braf$^{CA/+}$* spinal cord, pERK1/2+ (red) Aldh1L1-GFP+ (green) cells are significantly increased and quantified in E. (**F**) EdU injection timetable of *hGFAP-cre; Braf$^{CA/+}$* mice is shown and normalised fold change of EdU+ Aldh1L1-GFP+/Aldh1L1-GFP+ compared with littermate controls are quantified in three different domains. Grey bars represent control whereas white bars are for mutant animals. Statistical analyses are performed by *t*-test. **P*<0.05. Error bars represent s.d. Scale bars: 100 μm.

whether temporal regulation of BRAF^{V600E}-driven astrocyte precursor proliferation required p16^{Ink4a} and p19^{Arf} function during normal development, we analysed *hGFAP-cre; Braf$^{CA/+}$; Aldh1L1-GFP* mice that additionally lacked *Ink4a-Arf*, encoding p16^{Ink4a} and p19^{Arf}. As shown (Fig. 7D), at P7 <4% of normal (or *hGFAP-cre; Braf$^{CA/+}$; Ink4a-Arf$^{+/+}$; Aldh1L1-GFP* control animals) Aldh1L1-GFP cells are Ki-67-positive. By contrast, *BRAF^{V600E}* activation in conjunction with homozygous *Ink4a-Arf* deficiency resulted in double the rate of Aldh1L1-GFP cell proliferation at P7 (P<0.05). This effect of *Ink4a-Arf* deletion, however, is no longer detectable at P14 (Fig. 7E), suggesting that an additional checkpoint exists to keep astrocytes from re-entering the cell cycle. Together, these findings suggest that gain of BRAF^{V600E} function promotes excessive astrocyte expansion but that it respects the temporal proliferation window of normal astrocyte development, partly owing to the cyclin inhibitor/tumor suppressors p16^{Ink4a} and p19^{Arf}.

DISCUSSION

Astrocytes provide structural support, regulate water balance and ion distribution, and maintain the blood-brain barrier. Roles for astrocytes in synapse formation and regulation and in human neurological disorders, such as amyotrophic lateral sclerosis, epilepsy and astrocytoma, are a relatively recent discovery (Rowitch and Kriegstein, 2010; Zhang and Barres, 2010). Although astrocytes are the most numerous cell type in the CNS, remarkably little is known of the factors that regulate the ultimate size of astrocyte populations during development. Here, we trace the cellular and temporal origins of astrocytes in the spinal cord. Although our findings establish that the RAS signalling intermediate BRAF is an essential regulator of astrocyte precursor proliferation, they suggest additional complexity in the cell cycle regulatory mechanism that governs this process, including involvement of p16^{Ink4a} and/or p19^{Arf}.

Evidence that cellular origins of astrocytes vary across temporal epochs

Using the pan-lineage astrocyte marker *Aldh1L1-GFP*, we found extensive co-expression with radial glial markers commencing at E12.5-13.5 of mouse development, and that these Aldh1L1-GFP-positive progenitors gave rise to both protoplasmic astrocytes (PAs) and fibrous astrocytes (FAs). This is the first rigorous analysis of *Aldh1L1-GFP* expression in embryonic spinal cord. We found that reporter expression was restricted to glia predominantly of astrocyte lineage using the criteria of morphology and co-expression of the markers ALDOC and GFAP. In addition, we have observed that *Aldh1L1-cre* fate maps to astrocytes and some oligodendrocytes but few neurons (Fig. 1L-N). Together, these data indicate that the *Aldh1L1* expression commences in spinal cord radial glia at the time of their commitment to gliogenesis. Subsequently, *Aldh1L1-GFP* expression was observed almost exclusively in PA and FA but not oligodendrocytes or neurons, confirming its utility as an astrocyte pan-lineage marker (Cahoy et al., 2008).

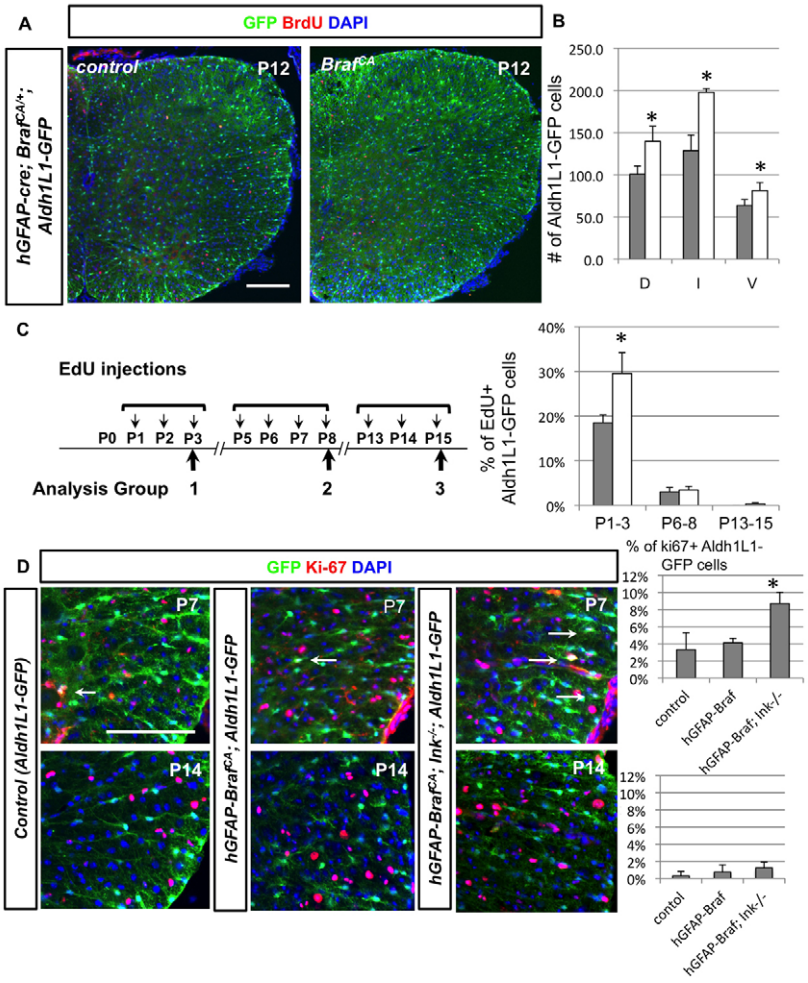

Fig. 7. Conditional BRAF^{V600E} animals do not exhibit increased proliferation potential in Aldh1L1-GFP+ cells after P5. (**A**,**B**) *hGFAP-cre; Braf$^{CA/+}$* animals were injection with BrdU at P7 and examined at P12. The total number of Aldh1L1-GFP+ cells in three domains is significantly increased (quantified in B). However, BrdU+ Aldh1L1-GFP+ cells in the mutant spinal cord are not increased compared with control animals. (**C**) Three EdU injections regimes and quantifications are shown. Increased proliferation of Aldh1L1-GFP+ cells in *hGFAP-cre; Braf$^{CA/+}$* spinal cord is only observed at the P1-3 time period but not in the P6-8 and P13-15 periods. Grey bars represent control whereas white bars are for mutant animals. (**D**) At P7 and P14, proliferation of astrocytes is assessed by percentage of Ki-67+ Aldh1L1-GFP+ cells in littermates of three genotypes, quantified in the bar graph: (1) *Braf$^{CA/+}$; Ink4a-Arf$^{+/+}$, Aldh1L1-GFP* (*control*), (2) *hGFAP-cre; Braf$^{CA/+}$; Ink4a-Arf$^{+/+}$, Aldh1L1-GFP* (*hGFAP-BRAF^{V600E}*) and (3) *hGFAP-cre; Braf$^{CA/+}$; Ink4a-Arf$^{-/-}$, Aldh1L1-GFP* (*hGFAP-BRAF^{V600E}; Ink$^{-/-}$*). Note that only at P7, loss of *Cdkn2a* locus shows significant effect on increasing astrocyte proliferation in *Braf^{CA}* animals. Statistical analyses are performed by *t*-test. **P*<0.05. Error bars represent s.d. Scale bars: 100 μm.

We used labelling with thymidine analogues coupled with *Aldh1L1-GFP* expression in both radial glia and discrete PA and FA astrocytes to determine the developmental epoch of astrocyte expansion. Our results indicate that proliferation of astrocyte progenitors is restricted to late embryonic and early neonatal stages in the spinal cord, which is in contrast to oligodendrocyte precursors (OLPs), which are produced in multiple waves in the CNS and continue to proliferate for the life of the animal at high rates (Cai et al., 2005; Fogarty et al., 2005; Vallstedt et al., 2005; Kessaris et al., 2006; Ligon et al., 2006). Astrocytes have been observed to proliferate at later stages after injury (Barnabé-Heider et al., 2010).

Identification of a putative intermediate amplifying astrocyte precursor cell

Our data is consistent with previous reports that astrocytes are derived from/expand via radial glial cells (Hirano and Goldman, 1988; Barry and McDermott, 2005), but they also suggest a further step in this process. Indeed, it is unclear whether expansion of astrocytes occurs solely by (1) symmetric expansion of radial glia and/or (2) production of intermediate proliferative (transit-amplifying) astrocyte precursors (IAPs), distinct from radial glia (Fig. 3E). In the developing forebrain and retina, putative IAPs (vimentin+, GFAP–) have been isolated that can differentiate into astrocytes (GFAP+) in vitro (Mi and Barres, 1999; Lin and Goldman, 2009). Recent in vivo studies from developing retina (Chan-Ling et al., 2009) and rat spinal cord (Barry and McDermott, 2005) also indicate that IAPs exist before radial glia fully differentiate into mature astrocytes.

However, proliferation of IAPs for CNS astrocytes has remained poorly characterised. By analysing several proliferative markers to label S-phase and mitotic Aldh1L1-GFP+ cells, we identified putative spinal cord IAPs in situ that extensively proliferate at E15-P3, beyond the phase of reporter expression in classic radial glial cells. Thus, we propose that ultimate astrocyte numbers are based on both transformation of radial glia as well as expansion of dispersed Aldh1L1-GFP-positive IAPs (Fig. 3E), a model comparable to the way certain neurons are derived indirectly from radial glia via IAPs in brain (Lui et al., 2011). Further studies, including gene expression profiling, are needed to identify markers specific to IAP populations in the spinal cord. Such studies might provide further information on whether IAPs represent a truly distinct stage from radial glia notwithstanding their clear morphological differences. Finally, we found that both Aldh1L1-GFP radial glia and IAPs cells from the intermediate and ventral spinal cord regions showed the highest proportion of proliferating astrocyte precursors at early stages, whereas dorsal proliferation was delayed (Fig. 3A-C). This suggests that domain-specific factors temporally regulate astrocyte proliferation, which could account for the relatively high astrocyte density in particular regions, such as the intermediate domain (Fig. 3). These findings are consistent with other domain-regulated developmental mechanisms that have been previously shown (Muroyama et al., 2005; Hochstim et al., 2008). However, further work is needed to distinguish whether the ultimate astrocytes populations in a region might also comprise cells that have migrated from other developmental domains.

BRAF signalling is necessary and sufficient to promote astrocyte precursor proliferation

In CNS development, ERK1/2 is a major component of the MAPK signalling cascade reported to regulate proliferation, growth and axonal pathfinding (Newbern et al., 2011). ERK1 and ERK2 loss of function in the nervous system affects neurogenesis in the forebrain, oligodendrocyte development in the CNS and myelination by Schwann cells in the PNS (Newbern et al., 2011). BRAF has been implicated in learning-memory in the hippocampus (Chen et al., 2006), sensory neuron axonal pathfinding and oligodendrocyte differentiation (Galabova-Kovacs et al., 2008). These findings are important for our understanding of the pathogenic outcomes underlying NCFC (neuro-cardio-facio-cutaneous) syndromes caused by aberrant ERK1/2 signalling (Tidyman and Rauen, 2009).

Here, we demonstrated that ERK1/2 activity is highly elevated in proliferating (Ki-67+) astrocytes. Genetic analysis of *Braf*, a key upstream regulator of ERK1/2, confirmed that regulation of BRAF signalling is crucial for normal astrocyte precursor proliferation in the spinal cord. Although further investigation is needed to determine the proliferative pathways that might explain why certain dorsoventral domains produce relatively high numbers of astrocytes, our data implicates BRAF signalling as a regulator of the overall proliferation process. In *Braf* mutants, astrocyte proliferation is moderately decreased by ~20%, suggesting additional crucial factors for astrocyte proliferation. This is not surprising given that BRAF is one of several redundant RAS signalling mediators. Further work is needed to determine whether removal of both BRAF and CRAF (RAF1 – Mouse Genome Informatics), for example, would more significantly disrupt astrocytic expansion.

In gain-of-function $BRAF^{V600E}$ mutants, increased proliferation of astrocyte precursors is evident during the normal time frame (E13.5-P3) of astrogliogenesis. Although we cannot rule out the possibility that non-autonomous effects of other cell types affect astrocyte proliferation (as both *Blbp-lacZ-cre* and *hGFAP-cre* lines target additional progeny types), we did observe an increased number of pERK1/2+ astrocyte precursors, suggesting that ectopic pERK1/2 activity in astrocyte precursors per se drives proliferation. We also observed that cultured astrocyte proliferation was stimulated by $BRAF^{V600E}$, further suggesting cell-autonomous effects of BRAF signalling. Finally, consistent with our findings, loss-of-function studies with neurofibromatosis 1 (NF1), a negative regulator of the ERK cascade, show increased GFAP-positive astrocyte number (Hegedus et al., 2007), suggesting that ERK activity also regulates glial proliferation in the brain.

What factors lie upstream of ERK activation in astrocytes? Signalling pathways including BMP, CNTF and NOTCH are regulators of astrocyte maturation and/or the developmental neuron-glia switch; thus, it would be of interest to investigate their mechanistic interactions with the ERK signalling axis. Previous analysis using immunopanning and microarray (Cahoy et al., 2008) indicates that EGFR is expressed in brain astrocytes. After isolating Aldh1L1-GFP+ cells from spinal cord of different developmental stages, we performed qPCR for EGFR expression and found that EGFR is indeed expressed in proliferating Aldh1L1-GFP+ cells during the course of E14-P7 (supplementary material Fig. S5). Together, these results suggest that EGFR is a possible candidate upstream of ERK signalling for regulation of astrocyte proliferation.

Evidence that mature astrocytes possess mechanisms to restrict the activity of mitogenic BRAF signalling

Elevated ERK activity resulting from BRAF mutation is aetiological in melanoma (Davies et al., 2002; Dankort et al., 2009), and a role for $BRAF^{V600E}$ in paediatric gliomagenesis is supported by several recent studies (Schiffman et al., 2010). Although our findings indicate that $BRAF^{V600E}$ is capable of promoting astrocyte hyperproliferation, it only does so during a tightly restricted temporal window (E13.5-P3). Similarly, expression of $BRAF^{V600E}$ in melanocytes and lung induces initial proliferation but eventually fails to progress to tumor formation (Dankort et al., 2007; Dankort et al., 2009). One possibility is that the astrocyte precursor response to $BRAF^{V600E}$ signalling is itself temporally restricted. In support of this, we see a loss of pERK1/2 expression in astrocytes at later stages commencing at P4 even for $hGFAP\text{-}Braf^{CA/+}$ animals.

In both melanoma and glioma, $BRAF^{V600E}$ mutation is often associated with homozygous deletion of *Ink4a-Arf*, suggesting that loss of *Ink4a-Arf* expression might be selected for in these cancers. When $hGFAP\text{-}Braf^{CA/+}$; $Ink4a\text{-}Arf^{-/-}$ animals were examined, a somewhat prolonged phase of proliferation in spinal cord astrocytes was achieved. This indicates that function of $p16^{Ink4a}$ and/or $p19^{Arf}$ is required in part to prevent $BRAF^{V600E}$-stimulated astrocytes from re-entering the cell cycle. However, because such astrocytes later do leave the cell cycle, additional checkpoints must exist. One possibility is that the astrocyte precursor response to $BRAF^{V600E}$ signalling is itself temporally restricted, which is supported by our observation pERK1/2 expression described above. This is in contrast with studies in lung where expression of $BRAF^{V600E}$ cooperates with loss of *Ink4a-Arf* to induce tumor formation (Dankort et al., 2007). This suggests distinct regulatory checkpoint mechanisms for BRAF signalling in different tissues.

Unlike the spinal cord, rodent adult forebrain neural stem cell populations of the subventricular zone and hippocampus retain certain radial glia characteristics, such as expression of nestin and vimentin, and they show ongoing proliferation and progeny generation (Menn et al., 2006; Kriegstein and Alvarez-Buylla, 2009). Thus, it will be important in future work to investigate roles for BRAF in regulation of proliferation in such germinal zones.

Acknowledgements

We are grateful to Amelie Griveau and Emmanuelle Huillard for expert technical help and helpful comments on the manuscript.

Funding

This work was supported by grants from the National Institute of Neurological Disorders and Stroke [NS059893 to D.H.R. and B.A.B.]; the National Cancer Institute [CA131261 to M.M., U01-CA141549 to D.H.G.]; and the American Medical Resources Foundation [to N.H.]. D.H.R. and N.H. are Howard Hughes Medical Institute Investigators. Deposited in PMC for release after 6 months.

Competing interests statement

The authors declare no competing financial interests.

Supplementary material

Supplementary material available online at
http://dev.biologists.org/lookup/suppl/doi:10.1242/dev.077214/-/DC1

References

Agius, E., Soukkarieh, C., Danesin, C., Kan, P., Takebayashi, H., Soula, C. and Cochard, P. (2004). Converse control of oligodendrocyte and astrocyte lineage development by Sonic hedgehog in the chick spinal cord. *Dev. Biol.* **270**, 308-321.

Alcantara Llaguno, S., Chen, J., Kwon, C. H., Jackson, E. L., Li, Y., Burns, D. K., Alvarez-Buylla, A. and Parada, L. F. (2009). Malignant astrocytomas originate from neural stem/progenitor cells in a somatic tumor suppressor mouse model. *Cancer Cell* **15**, 45-56.

Bachoo, R. M., Kim, R. S., Ligon, K. L., Maher, E. A., Brennan, C., Billings, N., Chan, S., Li, C., Rowitch, D. H., Wong, W. H. et al. (2004). Molecular diversity of astrocytes with implications for neurological disorders. *Proc. Natl. Acad. Sci. USA* **101**, 8384-8389.

Barnabé-Heider, F., Göritz, C., Sabelström, H., Takebayashi, H., Pfrieger, F. W., Meletis, K. and Frisén, J. (2010). Origin of new glial cells in intact and injured adult spinal cord. *Cell Stem Cell* **7**, 470-482.

Barry, D. and McDermott, K. (2005). Differentiation of radial glia from radial precursor cells and transformation into astrocytes in the developing rat spinal cord. *Glia* **50**, 187-197.

Cahoy, J. D., Emery, B., Kaushal, A., Foo, L. C., Zamanian, J. L., Christopherson, K. S., Xing, Y., Lubischer, J. L., Krieg, P. A., Krupenko, S. A. et al. (2008). A transcriptome database for astrocytes, neurons, and oligodendrocytes: a new resource for understanding brain development and function. *J. Neurosci.* **28**, 264-278.

Cai, J., Qi, Y., Hu, X., Tan, M., Liu, Z., Zhang, J., Li, Q., Sander, M. and Qiu, M. (2005). Generation of oligodendrocyte precursor cells from mouse dorsal spinal cord independent of Nkx6 regulation and Shh signaling. *Neuron* **45**, 41-53.

Chan-Ling, T., Chu, Y., Baxter, L., Weible, M., II and Hughes, S. (2009). In vivo characterization of astrocyte precursor cells (APCs) and astrocytes in developing rat retinae: differentiation, proliferation, and apoptosis. *Glia* **57**, 39-53.

Chen, A. P., Ohno, M., Giese, K. P., Kühn, R., Chen, R. L. and Silva, A. J. (2006). Forebrain-specific knockout of B-raf kinase leads to deficits in hippocampal long-term potentiation, learning, and memory. *J. Neurosci. Res.* **83**, 28-38.

Dankort, D., Filenova, E., Collado, M., Serrano, M., Jones, K. and McMahon, M. (2007). A new mouse model to explore the initiation, progression, and therapy of BRAFV600E-induced lung tumors. *Genes Dev.* **21**, 379-384.

Dankort, D., Curley, D. P., Cartlidge, R. A., Nelson, B., Karnezis, A. N., Damsky, W. E., You, M. J., DePinho, R. A., McMahon, M. and Bosenberg, M. (2009). Braf(V600E) cooperates with Pten loss to induce metastatic melanoma. *Nat. Genet.* **41**, 544-552.

Davies, H., Bignell, G. R., Cox, C., Stephens, P., Edkins, S., Clegg, S., Teague, J., Woffendin, H., Garnett, M. J., Bottomley, W. et al. (2002). Mutations of the BRAF gene in human cancer. *Nature* **417**, 949-954.

Deneen, B., Ho, R., Lukaszewicz, A., Hochstim, C. J., Gronostajski, R. M. and Anderson, D. J. (2006). The transcription factor NFIA controls the onset of gliogenesis in the developing spinal cord. *Neuron* **52**, 953-968.

Doyle, J. P., Dougherty, J. D., Heiman, M., Schmidt, E. F., Stevens, T. R., Ma, G., Bupp, S., Shrestha, P., Shah, R. D., Doughty, M. L. et al. (2008). Application of a translational profiling approach for the comparative analysis of CNS cell types. *Cell* **135**, 749-762.

Duesbery, N. and Vande Woude, G. (2006). BRAF and MEK mutations make a late entrance. *Sci. STKE* **2006**, pe15.

Fogarty, M., Richardson, W. D. and Kessaris, N. (2005). A subset of oligodendrocytes generated from radial glia in the dorsal spinal cord. *Development* **132**, 1951-1959.

Galabova-Kovacs, G., Catalanotti, F., Matzen, D., Reyes, G. X., Zezula, J., Herbst, R., Silva, A., Walter, I. and Baccarini, M. (2008). Essential role of B-Raf in oligodendrocyte maturation and myelination during postnatal central nervous system development. *J. Cell Biol.* **180**, 947-955.

Gong, S., Zheng, C., Doughty, M. L., Losos, K., Didkovsky, N., Schambra, U. B., Nowak, N. J., Joyner, A., Leblanc, G., Hatten, M. E. et al. (2003). A gene expression atlas of the central nervous system based on bacterial artificial chromosomes. *Nature* **425**, 917-925.

Gong, S., Doughty, M., Harbaugh, C. R., Cummins, A., Hatten, M. E., Heintz, N. and Gerfen, C. R. (2007). Targeting Cre recombinase to specific neuron populations with bacterial artificial chromosome constructs. *J. Neurosci.* **27**, 9817-9823.

Hegedus, B., Dasgupta, B., Shin, J. E., Emnett, R. J., Hart-Mahon, E. K., Elghazi, L., Bernal-Mizrachi, E. and Gutmann, D. H. (2007). Neurofibromatosis-1 regulates neuronal and glial cell differentiation from neuroglial progenitors in vivo by both cAMP- and Ras-dependent mechanisms. *Cell Stem Cell* **1**, 443-457.

Heintz, N. (2004). Gene expression nervous system atlas (GENSAT). *Nat. Neurosci.* **7**, 483.

Herculano-Houzel, S. (2009). The human brain in numbers: a linearly scaled-up primate brain. *Front. Hum. Neurosci.* **3**, 1-11.

Hirano, M. and Goldman, J. E. (1988). Gliogenesis in rat spinal cord: evidence for origin of astrocytes and oligodendrocytes from radial precursors. *J. Neurosci. Res.* **21**, 155-167.

Hochstim, C., Deneen, B., Lukaszewicz, A., Zhou, Q. and Anderson, D. J. (2008). Identification of positionally distinct astrocyte subtypes whose identities are specified by a homeodomain code. *Cell* **133**, 510-522.

Kessaris, N., Fogarty, M., Iannarelli, P., Grist, M., Wegner, M. and Richardson, W. D. (2006). Competing waves of oligodendrocytes in the forebrain and postnatal elimination of an embryonic lineage. *Nat. Neurosci.* **9**, 173-179.

Kettenmann, H. and Ransom, B. R. (2005). *Neuroglia*, 2nd edn. Oxford: Oxford University Press.

Kriegstein, A. and Alvarez-Buylla, A. (2009). The glial nature of embryonic and adult neural stem cells. *Annu. Rev. Neurosci.* **32**, 149-184.

Lee, K. J. and Jessell, T. M. (1999). The specification of dorsal cell fates in the vertebrate central nervous system. *Annu. Rev. Neurosci.* **22**, 261-294.

Ligon, K. L., Fancy, S. P., Franklin, R. J. and Rowitch, D. H. (2006). Olig gene function in CNS development and disease. *Glia* **54**, 1-10.

Lin, G. and Goldman, J. E. (2009). An FGF-responsive astrocyte precursor isolated from the neonatal forebrain. *Glia* **57**, 592-603.

Lloyd, A. C., Obermüller, F., Staddon, S., Barth, C. F., McMahon, M. and Land, H. (1997). Cooperating oncogenes converge to regulate cyclin/cdk complexes. *Genes Dev.* **11**, 663-677.

Lui, J. H., Hansen, D. V. and Kriegstein, A. R. (2011). Development and evolution of the human neocortex. *Cell* **146**, 18-36.

McCarthy, K. D. and de Vellis, J. (1980). Preparation of separate astroglial and oligodendroglial cell cultures from rat cerebral tissue. *J. Cell Biol.* **85**, 890-902.

Menn, B., Garcia-Verdugo, J. M., Yaschine, C., Gonzalez-Perez, O., Rowitch, D. and Alvarez-Buylla, A. (2006). Origin of oligodendrocytes in the subventricular zone of the adult brain. *J. Neurosci.* **26**, 7907-7918.

Mi, H. and Barres, B. A. (1999). Purification and characterization of astrocyte precursor cells in the developing rat optic nerve. *J. Neurosci.* **19**, 1049-1061.

Michaloglou, C., Vredeveld, L. C., Soengas, M. S., Denoyelle, C., Kuilman, T., van der Horst, C. M., Majoor, D. M., Shay, J. W., Mooi, W. J. and Peeper, D. S. (2005). BRAFE600-associated senescence-like cell cycle arrest of human naevi. *Nature* **436**, 720-724.

Molofsky, A. V., Pardal, R., Iwashita, T., Park, I. K., Clarke, M. F. and Morrison, S. J. (2003). Bmi-1 dependence distinguishes neural stem cell self-renewal from progenitor proliferation. *Nature* **425**, 962-967.

Muroyama, Y., Fujiwara, Y., Orkin, S. H. and Rowitch, D. H. (2005). Specification of astrocytes by bHLH protein SCL in a restricted region of the neural tube. *Nature* **438**, 360-363.

Nedergaard, M., Ransom, B. and Goldman, S. A. (2003). New roles for astrocytes: redefining the functional architecture of the brain. *Trends Neurosci.* **26**, 523-530.

Newbern, J. M., Li, X., Shoemaker, S. E., Zhou, J., Zhong, J., Wu, Y., Bonder, D., Hollenback, S., Coppola, G., Geschwind, D. H. et al. (2011). Specific functions for ERK/MAPK signaling during PNS development. *Neuron* **69**, 91-105.

Niihori, T., Aoki, Y., Narumi, Y., Neri, G., Cavé, H., Verloes, A., Okamoto, N., Hennekam, R. C., Gillessen-Kaesbach, G., Wieczorek, D. et al. (2006). Germline KRAS and BRAF mutations in cardio-facio-cutaneous syndrome. *Nat. Genet.* **38**, 294-296.

Oberheim, N. A., Takano, T., Han, X., He, W., Lin, J. H., Wang, F., Xu, Q., Wyatt, J. D., Pilcher, W., Ojemann, J. G. et al. (2009). Uniquely hominid features of adult human astrocytes. *J. Neurosci.* **29**, 3276-3287.

Pringle, N. P., Guthrie, S., Lumsden, A. and Richardson, W. D. (1998). Dorsal spinal cord neuroepithelium generates astrocytes but not oligodendrocytes. *Neuron* **20**, 883-893.

Rodriguez-Viciana, P., Tetsu, O., Tidyman, W. E., Estep, A. L., Conger, B. A., Cruz, M. S., McCormick, F. and Rauen, K. A. (2006). Germline mutations in genes within the MAPK pathway cause cardio-facio-cutaneous syndrome. *Science* **311**, 1287-1290.

Rowitch, D. H. and Kriegstein, A. R. (2010). Developmental genetics of vertebrate glial-cell specification. *Nature* **468**, 214-222.

Schiffman, J. D., Hodgson, J. G., VandenBerg, S. R., Flaherty, P., Polley, M. Y., Yu, M., Fisher, P. G., Rowitch, D. H., Ford, J. M., Berger, M. S. et al. (2010). Oncogenic BRAF mutation with CDKN2A inactivation is characteristic of a subset of pediatric malignant astrocytomas. *Cancer Res.* **70**, 512-519.

Schmechel, D. E. and Rakic, P. (1979). A Golgi study of radial glial cells in developing monkey telencephalon: morphogenesis and transformation into astrocytes. *Anat. Embryol. (Berl.)* **156**, 115-152.

Skoff, R. P., Price, D. L. and Stocks, A. (1976). Electron microscopic autoradiographic studies of gliogenesis in rat optic nerve. II. Time of origin. *J. Comp. Neurol.* **169**, 313-334.

Stiles, C. D. and Rowitch, D. H. (2008). Glioma stem cells: a midterm exam. *Neuron* **58**, 832-846.

Stolt, C. C., Lommes, P., Sock, E., Chaboissier, M. C., Schedl, A. and Wegner, M. (2003). The Sox9 transcription factor determines glial fate choice in the developing spinal cord. *Genes Dev.* **17**, 1677-1689.

The Cancer Genome Atlas Research Network (2008). Comprehensive genomic characterization defines human glioblastoma genes and core pathways. *Nature* **455**, 1061-1068.

Tidyman, W. E. and Rauen, K. A. (2009). The RASopathies: developmental syndromes of Ras/MAPK pathway dysregulation. *Curr. Opin. Genet. Dev.* **19**, 230-236.

Vallstedt, A., Klos, J. M. and Ericson, J. (2005). Multiple dorsoventral origins of oligodendrocyte generation in the spinal cord and hindbrain. *Neuron* **45**, 55-67.

Zambrowicz, B. P., Imamoto, A., Fiering, S., Herzenberg, L. A., Kerr, W. G. and Soriano, P. (1997). Disruption of overlapping transcripts in the ROSA beta geo 26 gene trap strain leads to widespread expression of beta-galactosidase in mouse embryos and hematopoietic cells. *Proc. Natl. Acad. Sci. USA* **94**, 3789-3794.

Zhang, Y. and Barres, B. A. (2010). Astrocyte heterogeneity: an underappreciated topic in neurobiology. *Curr. Opin. Neurobiol.* **20**, 588-594.

Table S1. Quantification of astrocyte proliferation in various genotypes

Genotype	Counted area	Average number of cells counted (*n*=3)	Age	EdU injections	Percentage	Normalized to 1
Aldh1L1-GFP	Half spinal cord	288	E18	E15-17	41.2	
		329	P3	P1-3	23.8	
		333	P8	P6-8	3.0	
Aldh1L1-GFP	Dorsal	34	E16	2 hours	7	
	Intermediate	57	E16	2 hours	21	
	Ventral	34	E16	2 hours	23	
Aldh1L1-GFP	Dorsal	65	E18	2 hours	11	
	Intermediate	141	E18	2 hours	13	
	Ventral	61	E18	2 hours	15	
Braf KO control	Dorsal	63	E18	E15-17	29	1
	Intermediate	157	E18	E15-17	41.30	1
	Ventral	67.7	E18	E15-17	52	1
Braf KO mutant	Dorsal	47	E18	E15-17	27	0.92
	Intermediate	133	E18	E15-17	34	0.83
	Ventral	61.3	E18	E15-17	44	0.84
Braf KO control	Dorsal	115	P8	E16-18	14	1
	Intermediate	152	P8	E16-18	34	1
	Ventral	69	P8	E16-18	48	1
Braf KO mutant	Dorsal	91	P8	E16-18	14	1
	Intermediate	139	P8	E16-18	25	0.72
	Ventral	73.3	P8	E16-18	34	0.72
Braf KO control	Dorsal	99	P3	P1-3	23	1
	Intermediate	174	P3	P1-3	21	1
	Ventral	75	P3	P1-3	28	1
Braf KO mutant	Dorsal	94	P3	P1-3	20	0.85
	Intermediate	161	P3	P1-3	17	0.83
	Ventral	80	P3	P1-3	24	0.87
Braf-CA control	Dorsal	73	E18	E15-17	14	1

	Intermediate	123	E18	E15-17	20	1
	Ventral	65	E18	E15-17	29	1
Braf-CA mutant	Dorsal	88	E18	E15-17	18	1.3
	Intermediate	142	E18	E15-17	30	1.48
	Ventral	71.3	E18	E15-17	37	1.27
Braf-CA control	Dorsal	117	P3	P1-3	17	1
	Intermediate	167	P3	P1-3	21	1
	Ventral	80.7	P3	P1-3	19	1
Braf-CA mutant	Dorsal	132	P3	P1-3	21	1.23
	Intermediate	191	P3	P1-3	29	1.37
	Ventral	90.7	P3	P1-3	27	1.44
Braf-CA control	WM	86	P7		3.30	
Braf-CA mutant	WM	121	P7		4.10	
Braf-CA Ink–/–	WM	96	P7		8.70	
Braf-CA control	WM	103	P14		0.91	
Braf-CA mutant	WM	143	P14		1.67	
Braf-CA Ink–/–	WM	112	P14		1.23	